Strain Hardening in Polymer Glasses: Limitations of Network Models

Robert S. Hoy* and Mark O. Robbins

Department of Physics and Astronomy, Johns Hopkins University, Baltimore, Maryland 21218, USA

(Received 25 May 2007; published 14 September 2007)

Simulations are used to examine the microscopic origins of strain hardening in polymer glasses. While traditional entropic network models can be fit to the total stress, their underlying assumptions are inconsistent with simulation results. There is a substantial energetic contribution to the stress that rises rapidly as segments between entanglements are pulled taut. The thermal component of stress is less sensitive to entanglements, mostly irreversible, and directly related to the rate of local plastic rearrangements. Entangled and unentangled chains show the same strain hardening when plotted against the microscopic chain orientation rather than the macroscopic strain.

DOI: 10.1103/PhysRevLett.99.117801 PACS numbers: 61.41.+e, 61.43.−j, 81.05.Lg

The stress needed to deform a polymer glass increases as the strain rises. This strain hardening plays a critical role in stabilizing polymers against strain localization and fracture, and reduces wear [1]. While models have had some success in fitting experimental data, fundamental inconsistencies in fit parameters and trends imply that our understanding of the microscopic origins of strain hardening is far from complete.

Most theories of strain hardening [2,3] are based on rubber elasticity theory [4]. These entropic network models assume that polymer glasses behave like cross-linked rubber, with the number of monomers between cross-links equal to the entanglement length N_e. The increase in the stress σ due to deformation by a stretch tensor $\bar{\lambda}$ is attributed to the decrease in entropy as polymers are stretched between affinely displaced entanglements. One finds [3]

$$\sigma(\bar{\lambda}) = \sigma_0 + G_R g(\bar{\lambda}) L^{-1}(h)/3h, \tag{1}$$

where σ_0 is the yield or plastic flow stress, G_R is the strain hardening modulus, L^{-1} is the inverse Langevin function, $g(\bar{\lambda})$ describes the entropy reduction for Gaussian chains, and $L^{-1}(h)/3h$ corrects for the finite length of segments between entanglements. The value of N_e enters in h, which is the ratio of the Euclidean distance between entanglements to the contour length.

Stress-stretch curves for a wide variety of glassy polymers can be fit to Eq. (1), but the fit parameters are not consistent with the microscopic picture underlying entropic network models [5]. For example, values of N_e from fitting h may be several times smaller than those obtained from the plateau modulus G_N^0 [3]. Entropic network models predict $G_R \approx G_N^0$ near T_g, but measured G_R are about 100 times larger [6]. G_R also rises as T decreases [6,7], while any entropic stress must drop to zero as $T \to 0$ [5]. Recent work [7,8] shows that changes in G_R correlate with those in the plastic flow stress. Indeed, entire stress-stretch curves collapse when normalized by σ_0 [7]. This is not expected from entropic models, where σ_0 is treated as an independent parameter arising from local plasticity. A more conceptual difficulty in entropic models is that, unlike rubber, glasses are not able to dynamically sample chain conformations.

In this Letter we use simulations to examine the microscopic origins of strain hardening. While our results for the total stress can be fit to Eq. (1), network models are not consistent with observed changes in energy, heat flow, and molecular conformations. The stress can be divided into energetic and thermal contributions. The energetic contribution is strictly zero in the entropic model, but we find it becomes significant as the segments between entanglements are stretched taut. In contrast, entanglements have little direct influence on the thermal contribution. This thermal stress is found to be directly related to the rate of local plastic rearrangements. Finally, network models only predict strain hardening for entangled chains, yet substantial hardening is observed for chains as small as $N_e/4$. Results for entangled and unentangled chains collapse when plotted as a function of the microscopic strain-induced orientation of chains rather than the macroscopic strain.

Much of the physics of polymer glasses is independent of chemical detail [3,9,10]. We thus employ a simple coarse-grained bead-spring model [11] that captures the key physics of linear homopolymers. Each polymer chain contains N beads of mass m. All beads interact via the truncated and shifted Lennard-Jones potential $U_{\mathrm{LJ}}(r) = 4u_0[(a/r)^{12} - (a/r)^6 - (a/r_c)^{12} + (a/r_c)^6]$, where $r_c = 1.5a$ is the cutoff radius and $U_{\mathrm{LJ}}(r) = 0$ for $r > r_c$. We express all quantities in terms of the molecular diameter a, binding energy u_0, and characteristic time $\tau_{\mathrm{LJ}} = \sqrt{ma^2/u_0}$. Mappings to real polymers give τ_{LJ} in the picosecond range [11].

Covalent bonds between adjacent monomers on a chain are modeled using the finitely extensible nonlinear elastic potential $U(r) = -(1/2)(kR_0^2)\ln[1 - (r/R_0)^2]$, with the canonical parameter choices $R_0 = 1.5a$ and $k = 30u_0/a^2$ [11]. Chain stiffness is introduced through a bending potential $U_{\mathrm{bend}}(\theta) = k_{\mathrm{bend}}(1 - \cos\theta)$, where θ is the angle between consecutive covalent bond vectors along a chain. Stiffer chains have lower entanglement lengths. Values of

 © 2007 The American Physical Society

N_e obtained from primitive path analysis (PPA) [12] range from $N_e = 71$ for flexible chains ($k_{\text{bend}} = 0$) to $N_e = 22$ for $k_{\text{bend}} = 2.0u_0$.

Glassy states were obtained by rapid temperature quenches from well-equilibrated melts [13] to a temperature T below the glass transition temperature $T_g \simeq 0.35u_0/k_B$ [14]. While quench rate affects the initial yield stress [15], it has little influence on strain hardening. Periodic boundary conditions were imposed, with periods L_i along directions $i = x$, y, and z. The initial periods L_i^0 were chosen to give zero pressure at T. A Langevin thermostat with damping rate $1/\tau_{\text{LJ}}$ was applied to the peculiar velocities in all three directions.

Experiments commonly impose compressive deformations because they suppress strain localization [6,10,16]. Simulations were performed for both uniaxial and plane strain compression. Both show the same behavior, and only uniaxial results are presented below. The cell is compressed along z at constant true strain rate $\dot{\epsilon} = \dot{L}_z/L_z = 10^{-5}/\tau_{\text{LJ}}$. While experimental rates are much lower, they show a weak logarithmic rate dependence. We find the same weak variation up to $\dot{\epsilon} = -10^{-3}/\tau_{\text{LJ}}$. Qualitative changes can occur at the higher rates employed in recent atomistic simulations of strain hardening [17–19]. The stress perpendicular to the compressive axis is maintained at zero by varying L_x and L_y [20]. Fits to network models normally assume that the volume remains constant and $L_x = L_y$, and this is approximately true in our simulations. Then deformation can be expressed in terms of a single stretch component $\lambda \equiv L_z/L_z^0$.

Typical strain hardening results are shown in Fig. 1. As in experiments, the stress is plotted against $g(\lambda) \equiv \lambda^2 - 1/\lambda$. Then entropic network models [Eq. (1)] attribute curvature in the strain hardening regime ($|g| \gtrsim 0.5$) to reductions in entropy associated with the finite length N_e between entanglements. The strong upward curvature in Fig. 1 can be fit to Eq. (1) (dotted line), but with a value of $N_e = 13$ that is much smaller than that determined from G_N^0 or PPA ($N_e = 22$). Similar reductions are found for other chain stiffnesses and in fits to experiment.

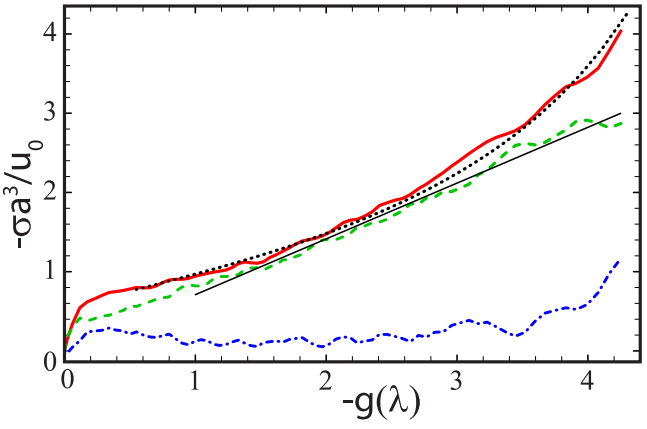

FIG. 1 (color online). Total stress (solid line) and contributions from heat (dashed line) and potential energy (dot-dashed line) for a system with $T = 0.2u_0/k_B$, $N = 350$, and $N_e = 22$. Fits of σ to Eq. (1) with $N_e = 13$ (dotted line) and of σ_Q to a straight line are also shown. Both σ and g are negative under compression.

The stress represents the incremental work done on a unit volume of the system by an incremental strain. It can be divided into contributions from changes in the internal energy density U and the heat flow out of a unit volume Q: $\sigma = \sigma_U + \sigma_Q$ where $\sigma_U = \partial U/\partial\epsilon$ and $\sigma_Q = \partial Q/\partial\epsilon$. The derivation of Eq. (1) assumes that σ_U does not contribute to strain hardening and that σ_Q is entirely due to reversible heat associated with changes in entropy. Simulations allow these assumptions to be tested.

Figure 1 shows that results for σ_Q can be fit to the linear behavior predicted for the entropy of ideal Gaussian chains at $|g| > 1$. Fits to smaller $|g|$ can be obtained with $N_e = 30$ in Eq. (1), but fits to uniaxial and plane strain results always give N_e that are larger than values obtained from G_N^0 and PPA, and much larger than values from fits to the total stress. Separate simulations show that σ_Q is dominated by irreversible heat flow rather than changes in entropy. After straining to a large $|g|$ the stress is returned to zero. The stretch only relaxes about 10% and only ~5% of the work associated with σ_Q is recovered. Similar irreversibility is observed in experiments [16], confirming that the force cannot be entropic.

The energetic contribution to the stress in Fig. 1 is important during the initial rise to the plastic flow stress σ_0. The value of σ_U then drops to a small constant for $0.5 < |g| < 2.5$. At larger strains there is a pronounced upturn in σ_U that contributes almost all of the curvature in the total stress. This energetic term thus has a crucial effect on fit values of N_e even though the derivation of Eq. (1) assumes $\sigma_U = 0$. Similar results are found for all T and k_{bend}, and for plane strain. In all cases, σ_Q exhibits nearly ideal Gaussian behavior [$L^{-1}(h)/3h \simeq 1$] and σ_U leads to a more rapid rise in stress at large stretches. The effect of σ_U increases and extends to smaller $|g|$ as the value of N_e from PPA decreases.

Examination of the evolving conformations of individual chains also provides a test of entropic network models. If entanglements act like cross-links, then polymer glasses should deform affinely on scales greater than the entanglement spacing. Our recent studies confirm this affine displacement, and the associated increase in h as segments between entanglements pull taut [7]. Figure 1 shows that this increase in h has little effect on the thermal stresses that motivated Eq. (1). Instead, straightening of segments produces large energetic terms by disrupting the local packing structure. Energy is stored in increasing tension in the covalent bonds countered by compression of intermolecular bonds [21]. Experiments also find significant energy storage [16], and could in principal track σ_U over the full strain hardening regime.

Further insight into strain hardening is provided by examining the dependence on chain length. Entropic net-

work models assume that the length should not matter for highly entangled systems, $N \gg N_e$, and there should be no network to produce strain hardening for $N < N_e$. These ideas are difficult to test experimentally since samples with $N < N_e$ undergo brittle fracture at small strains [9]. Simulations confirm that σ is independent of N for $N \gg N_e$, but show substantial strain hardening for $N < N_e$ [7,17]. Figure 2(a) illustrates this hardening for chains as short as $N_e/4$. Results for short chains follow the asymptotic behavior of highly entangled chains ($N/N_e > 4$) to larger $|g|$ as N increases. This suggests that deformation changes chain conformations on longer scales as $|g|$ increases and that entanglements become relevant only at large $|g|$ ($|g| \gtrsim 2.5$ in Fig. 2).

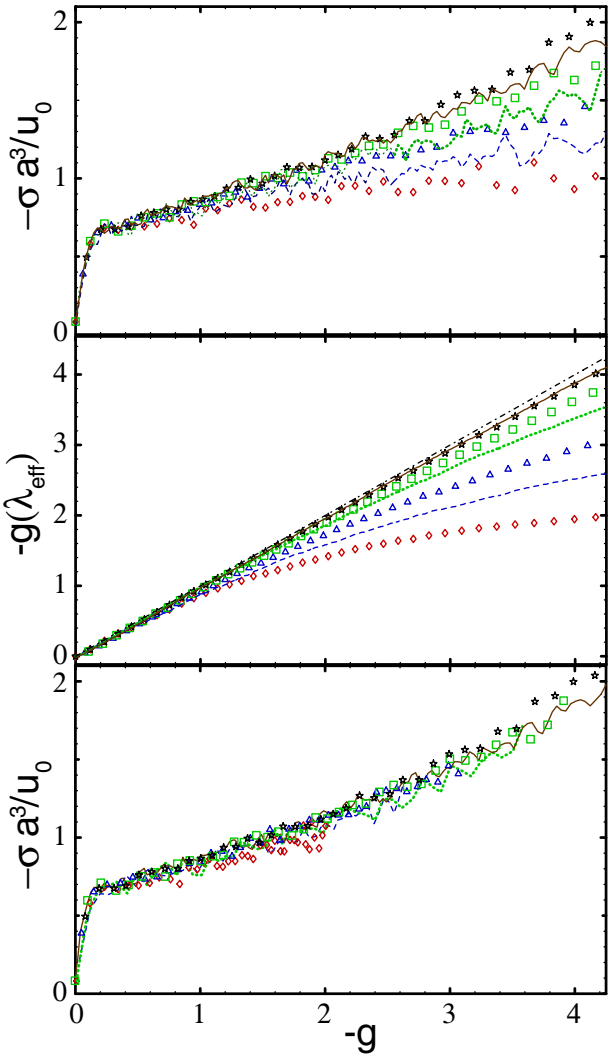

FIG. 2 (color online). (a) Stress versus $g(\lambda)$ during uniaxial compression at $k_BT = 0.2u_0$ for $k_{\text{bend}} = 0.75u_0$, $N_e = 39$, and strain rate $\dot{\epsilon} = -10^{-5}/\tau_{\text{LJ}}$. Successive curves from bottom to top are for $N = 10$ (◇), 16 (dashed line), 25 (△), 40 (dotted line), 70 (squares), 175 (solid line), and 350 (stars). (b) $g(\lambda_{\text{eff}})$ vs $g(\lambda)$ for the same systems. The dot-dashed line corresponds to $\lambda_{\text{eff}} = \lambda$. (c) Stresses for different N collapse when plotted against $g(\lambda_{\text{eff}})$.

The observation of strain hardening implies that the microscopic arrangement of chains evolves under stretching. One way of quantifying this is through changes in the root mean squared components R_i of the end-to-end vectors of chains relative to their initial values R_i^0. While the deformation of short chains is smaller than would be implied by the macroscopic stretch [7,22], we find that the changes in R_i are consistent with an effective volume conserving stretch λ_{eff} [23]. For uniaxial compression $\lambda_{\text{eff}} \equiv R_z/R_z^0 = (R_x^0/R_x)^2 = (R_y^0/R_y)^2$, where the last two equalities are implied by volume conservation [24]. Figure 2(b) shows $g(\lambda_{\text{eff}})$ as a function of $g(\lambda)$ for different N. All chains show significant stretching, and highly entangled systems deform affinely. The small deviation between $g(\lambda)$ and $g(\lambda_{\text{eff}})$ for $N \gg N_e$ results from a small increase in density ($\sim 4\%$) at large $|g|$ rather than nonaffine deformation. As N decreases, the deformation becomes subaffine at smaller and smaller $|g|$. This confirms that the scale over which chain conformations are distorted grows with $|g|$, and that entanglements become important only for $|g| \gtrsim 2.5$ in this system.

Strain hardening is directly related to the changes in chain conformation represented by λ_{eff} rather than the macroscopic deformation λ [23]. To illustrate this, data from Fig. 2(b) are replotted against $g(\lambda_{\text{eff}})$ in Fig. 2(c). Data for different chain lengths collapse onto a single curve even though N is as much as 4 times smaller than N_e. Similar results are found for other T, N_e, and for plane strain compression. Deviations are only seen when N becomes less than a few persistence lengths and chains can no longer be viewed as Gaussian random walks. These results show that entanglements do not have a direct effect on the thermal component of strain hardening. Their main role appears to be in forcing the local stretching of chains λ_{eff} to follow the global stretch λ.

The recently observed [7,8] correlation between the strain hardening modulus G_R and the plastic flow stress σ_0 suggests that local plastic rearrangements dissipate most of the energy during compression. To monitor the rate of plasticity $P \equiv \delta f/\delta\epsilon$, we counted the fraction δf of Lennard-Jones bonds with $r < r_c$ whose length changed by more than 20% over small intervals in strain $\delta\epsilon = 0.005$. Tests on this and related amorphous models [25] show that this criterion is large enough to exclude elastic deformations, and that $\delta\epsilon$ is small enough that a given bond does not undergo multiple events. To eliminate plastic rearrangements associated with equilibrium aging, the rate of plasticity during deformation was monitored at $T = 0$.

Figure 3 shows the rate of plasticity for $N_e = 26$ and 71. There is a rapid initial rise as σ approaches σ_0, followed by a nearly linear increase during the strain hardening regime. Also plotted in Fig. 3 are results for σ_Q. A fixed vertical rescaling (coincidentally close to unity in our units) produces an excellent collapse of P and σ_Q for all N_e. Note that even the fluctuations in the quantities are correlated

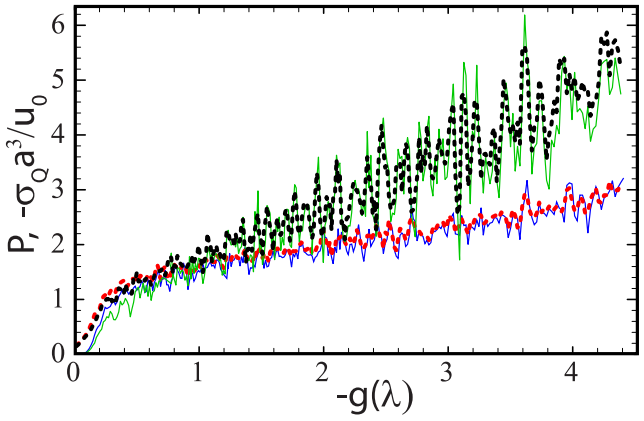

FIG. 3 (color online). Rate of plastic rearrangements P (solid lines) as a function of $g(\lambda)$ for $N_e = 26$, $N = 350$ (upper curve) and $N_e = 71$, $N = 500$ (lower curve) at $k_BT = 0u_0$. Dashed lines show the corresponding dissipative stress σ_Q.

[26]. Similar results are found for other criteria for the rate of plasticity, with only the scaling factor changing.

The above results clearly illustrate that the thermal contribution to strain hardening is associated with an increase in the rate of plastic rearrangements as chains stretch. It remains unclear why this increase should have the same functional form as the entropic stress of Gaussian chains (i.e., linear in $|g|$). The entropic stress represents the rate of decrease in the logarithm of the number of available chain conformations. One possibility is that the rate of plastic rearrangements scales in the same way because a decrease in the number of conformations necessitates larger scale plastic rearrangements. The relationship between the plastic flow stress and hardening modulus follows naturally from this picture, and it also explains why data for different chain lengths collapse when plotted against λ_{eff}. Analytic investigations of this scenario may prove fruitful.

Our results for σ_U suggest that the success of Eq. (1) in fitting the total stress may be coincidental, and explain why fit values of N_e are generally smaller than values from G_N^0 and PPA. It would be interesting to compare trends in the calculated σ_U and σ_Q to experimental results. These could be obtained by differentiating deformation calorimetry results for the work and heat, but existing studies have only extended to the plastic flow regime [27–29].

This material is based upon work supported by the National Science Foundation under Grant No. DMR-0454947. We thank G. S. Grest for providing equilibrated states and K. S. Schweizer and S. S. Sternstein for useful discussions. Simulations were performed with the LAMMPS software package [30].

*robhoy@pha.jhu.edu

[1] Y. J. Mergler and R. P. Schaake, J. Appl. Polym. Sci. **92**, 2689 (2004).
[2] R. N. Haward and G. Thackray, Proc. R. Soc. A **302**, 453 (1968).
[3] E. M. Arruda and M. C. Boyce, Int. J. Plast. **9**, 697 (1993).
[4] L. R. G. Treloar, *The Physics of Rubber Elasticity* (Clarendon, Oxford, 1975).
[5] E. J. Kramer, J. Polym. Sci., Part B: Polym. Phys. **43**, 3369 (2005).
[6] H. G. H. van Melick, L. E. Govaert, and H. E. H. Meijer, Polymer **44**, 2493 (2003).
[7] R. S. Hoy and M. O. Robbins, J. Polym. Sci., Part B: Polym. Phys. **44**, 3487 (2006).
[8] R. B. Dupaix and M. C. Boyce, Polymer **46**, 4827 (2005).
[9] *The Physics of Glassy Polymers*, edited by R. N. Haward and R. J. Young (Chapman and Hall, London, 1997), 2nd ed.
[10] R. N. Haward, Macromolecules **26**, 5860 (1993).
[11] K. Kremer and G. S. Grest, J. Chem. Phys. **92**, 5057 (1990).
[12] R. Everaers, S. K. Sukumaran, G. S. Grest, C. Svaneborg, A. Sivasubramanian, and K. Kremer, Science **303**, 823 (2004).
[13] R. Auhl, R. Everarers, G. S. Grest, K. Kremer, and S. J. Plimpton, J. Chem. Phys. **119**, 12 718 (2003).
[14] J. Rottler and M. O. Robbins, Phys. Rev. E **68**, 011507 (2003).
[15] J. Rottler and M. O. Robbins, Phys. Rev. Lett. **95**, 225504 (2005).
[16] O. A. Hasan and M. C. Boyce, Polymer **34**, 5085 (1993).
[17] A. V. Lyulin, N. K. Balabaev, M. A. Mazo, and M. A. J. Michels, Macromolecules **37**, 8785 (2004).
[18] At sufficiently high rates, chains are constrained to deform affinely. This gives $\lambda_{\text{eff}} = \lambda$ and the shear stress is nearly independent of $\dot{\epsilon}$. Thus the conclusion that strain hardening is controlled by λ_{eff} also applies in this limit.
[19] A. V. Lyulin, B. Vorselaars, M. A. Mazo, N. K. Balabaev, and M. A. J. Michels, Europhys. Lett. **71**, 618 (2005).
[20] L. Yang, D. J. Srolovitz, and A. F. Yee, J. Chem. Phys. **107**, 4396 (1997).
[21] C. Chui and M. C. Boyce, Macromolecules **32**, 3795 (1999).
[22] M. Dettenmaier, A. Maconnachie, J. S. Higgins, H. H. Kaush, and T. Q. Nguyen, Macromolecules **19**, 773 (1986).
[23] Our simulation study of λ_{eff} was motivated by its connection to strain hardening in a microscopic theory by K. Chen and K. S. Schweizer (private communication).
[24] When chains become shorter than a few persistence lengths, deviations from these last equalities become apparent and the best collapse is obtained by defining λ_{eff} from the expanded directions x and y. R. S. Hoy and M. O. Robbins, arXiv:0709.0769.
[25] B.-Q. Luan and M. O. Robbins (unpublished).
[26] A similar collapse is not achieved for the total stress, which has smaller fluctuations.
[27] G. W. Adams and R. J. Ferris, J. Polym. Sci., Part B: Polym. Phys. **26**, 433 (1988).
[28] O. B. Salamatina, G. W. H. Höhne, S. N. Rudnev, and E. F. Oleinik, Thermochim. Acta **247**, 1 (1994).
[29] E. F. Oleinik, S. N. Rudnev, O. B. Salamatina, S. V. Shenogin, M. I. Kotelyanskii, T. V. Paramzina, and S. I. Nazarenko, e-polymers **029** (2006).
[30] http://lammps.sandia.gov